# Clopyralid degradation by AOPs enhanced with zero valent iron

M.B. Ferreira[1,+], F.L. Souza[2], M. Muñoz-Morales[2,+], C. Sáez[2], P. Cañizares[2], C.A. Martínez-Huitle[1], M.A. Rodrigo[2,*]

[1] Institute of Chemistry, Federal University of Rio Grande do Norte, Campus Universitario 3000, 59078-970 Natal-RN, Brazil

[2] Department of Chemical Engineering, Faculty of Chemical Sciences and Technologies, University of Castilla-La Mancha, Campus Universitario s/n. 13071 Ciudad Real, Spain

**Abstract**

Four different technologies have been compared (photolysis, ZVI+ photolysis, electrolysis and ZVI + electrolysis) regarding the: (1) degradation of clopyralid, (2) extent of its mineralization, (3) formation of by-products and main reaction pathways. Results show that photolysis is the less efficient treatment and it only attains 5 % removal of the pollutant, much less than ZVI, which reaches 45% removal and that electrolysis, which attains complete removal and 78% mineralization within 4h. When ZVI is used as pre-treatment of electrolysis, it was obtained the most efficient technology. The identification of transformation products was carried out for each treatment by LC-MS. In total, ten products were identified. Tentative pathways for preferential clopyralid degradation for all processes were proposed. This work draws attention of the synergisms caused by the coupling of techniques involving the treatment of chlorinated compound and sheds light on how the preferential mechanisms of each treatment evaluated occurred.

**Keywords**

**Highlights**

- Oxidation capacity increases in the sequence: UV < ZVI + UV < EO < ZVI + EO.

- Higher rates of herbicides and mineralization were obtained in hybrid processes.

- High synergistic coefficients were obtained for the coupling of ZVI to UV and EO.

- Transformation products of clopyralid for each treatment have been identified

- Degradation pathways of clopyralid for each treatment evaluated were proposed.

*author to whom all correspondence should be addressed: manuel.rodrigo@uclm.es

+both authors contribute equally

## 1. Introduction

In the recent years, it has emerged an increasing interest in the application of advanced oxidation processes (AOPs) to deplete chlorinated hydrocarbons that have been widespread in the environment, because of their use as pesticides, degreasing agents or solvents. Among the technologies evaluated, it is important to highlight the electrochemical advanced oxidation processes (EAOPs), which have experienced great advances with the development of new electrodes materials, different processes and cells configurations, always searching for in order to increasing the cost-effectiveness of the treatments [1-4]. However, general drawbacks of these technologies are still those related to the high costs of electrode materials and the high power consumption required. To face these drawbacks, special design of cells looking for narrower electrode gaps and higher turbulences are looked for. Alternatively in some cases, it is proposed the addition of salts to the supporting electrolyte in order to increase the ionic conductivity, although this is not a sustainable choice because it leads to another type of pollution less hazardous but more persistent [5]. For these reasons, lots of studies have shown different alternatives to develop highly efficient electrochemical processes, based on the use of a combination of technologies that can improve the treatments in terms of economy. The coupling of electro-oxidation with concentration technologies reduces the negative impact of the mass transfer limitations on the efficiency. Among the novel technologies, it is worth to mention the electrocoagulation process (EC) that concentrates the colloid pollutants into flocs, reducing the volume of waste to be treated and making more efficient the later electrolysis [6, 7]. It is also important the novel electrochemical cells that integrate the concentration of ionic organics by electrodialysis with their electrooxidation [8, 9]. Finally regarding these novel concentration technologies, it has

65  also been proposed an adsorption process with granular active carbon (GAC) that allows

66  to concentrate the pollutants in methanol, from which they can be efficiently electrolyzed

67  [10]. This later technology  has also been successfully applied to remove gaseous

68  pollutants, such as perchloroethylene [11].

69  Thereby, electrochemical technologies can be integrated in other processes that promote

70  the indirect oxidation mechanisms, including UV light irradiation [12-14] or the

71  applications of ultrasounds [15] to stimulate the formation of large amount of oxidants

72  and free radicals, increasing the active substances that can react with the pollutants [16-

73  18]. Additionally, to increase the efficiency, other studies have considered the use of

74  reductive pathways using carbonaceous cathodes to produce hydrogen peroxide [19].

75  These systems increase their efficiency by using pressurized systems or combining with

76  catalysts (electro-Fenton (EF) processes) [20]. Besides, they have demonstrated to be

77  successful even in the integral treatment of anaerobic sludge [21] and in the treatment of

78  soil . With these novelties, it was developed a prototype for the efficient treatment of

79  soil washing wastes [22]. Considering other reductive pathways, many authors have

80  studied the hydro-dechlorination, that appears as an efficient technology under mild

81  reaction conditions (room temperature and atmospheric pressure). This non-

82  electrochemical process does not remove the pollutant but reduces its hazardousness and

83  toxicity [23]. It requires expensive catalysts (including ZVI) and continuous bubbling of

84  hydrogen. Because of that, in order to obtain a cheaper method and more easily

85  integrated with other technologies, the use of zero valent iron (ZVI) in combination with

86  electrolysis has emerged as a promising alternative. Successful results in the

87  dechlorination were reported for short chain chlorinated paraffins [24], lindane [25] or

88  trichloroethene [26], with studies included the evaluation of the intermediates generated

89  and the possible degradation pathways. Regarding electrochemical processes, in previous

90  works of our group ~~about the combination of this technology with EAOPs,~~ it was

91  demonstrated that~~, from the viewpoint of electrochemical treatment~~, a pre-treatment with

92  ZVI does not show important advantages regardless of the electrode material used and

93  the size of the ZVI particles [27]. However, it was confirmed great improvements in

94  biological treatability and toxicity of effluents after the application of these technologies

95  [28]. In order to clarify the mechanism of the removal of chlorinated hydrocarbons,

96  various authors have detailed reaction product formation using a photocatalytic

97  degradation in $TiO_2$ suspensions [29] and low pressure $UV/H_2O_2$ treatment [30]. Recent

98  studies report excellent results in the removal of persistent organic pollutants following

99  the use of combined systems with the use of ZVI and electro-oxidation technology, as

100  regards discharging standards, [31] biodegradability and toxicity [32] Furthermore, a

101  system using a Fe foam (Fe-F) was used as catalyst in the presence of tripolyphosphate

102  electrolyte (TPP) for electro-Fenton (EF) at neutral pH, allowed an 8.55-fold increase in

103  the rate of phenol degradation [33]. Nevertheless, to the best of our knowledge, there are

104  no fundamental studies of the different degradation pathways which can result from the

105  combination of ZVI dechlorination with AOPs technologies, such as photolysis or

106  electro-oxidation

107  In this work, we compared the removal efficiency of a well-known herbicide, clopyralid

108  (CLP), a polar organochlorinated compound effectively used to control annual and

109  perennial broadleaf weeds, with two AOPs technologies, photolysis and diamond

110  electrolysis, operated alone or coupled with a previous dehalogenation process with

111  micro particles of ZVI. In this line, some of the most recent works related to the removal

112  of CLP are summarized in Table 1 for the sake of comparison with the results that will

113  be presented in this work.

114  Table 1. Different alternatives to the Treatment of Clopyralid wastes using a coupled process.

| Method | Contaminant Concentration | Experimental Conditions | Removal | Ref |
|---|---|---|---|---|
| ZVI and soil-washing electrolysis | 30 mg $L^{-1}$ | ZVI = 48g and 72g; BDD anode and stainless steel cathode; T: 40º C; V: 2 L; J = 25 mA $cm^{-2}$. | Complete. | [34] |
| Electro-Fenton | 180 mg $L^{-1}$ | $Fe^{2+}$ = 0,1; 0,5; 1,2 and 5 mM; Platinum anode and carbon felt cathode; T = 20°C; V = 0,8 L, J = 50; 100, 200 and 300 mA. | 80% of removal. | [35] |
| Low pressure UV/$H_2O_2$ | 20 mg $L^{-1}$ | λ =254 nm; [$H_2O_2$] = 60 mg $L^{-1}$; V= 55 mL; Room temperature.. | 56% of removal. | [36] |
| UV/$H_2O_2$ and ozone oxidation | 0.078, 0.260, 0.391 and 0.521 mmol $L^{-1}$ | [$H_2O_2$] = 1g $L^{-1}$ and 2 g $L^{-1}$ V = 200 mL; T = at 25 ± 2 °C. | Complete removal with UV/$TiO_2$. | [37] |
| Photoelectrochemical oxidation and Sonoelectrochemical oxidation | 0.02 mg $g^{-1}$ | BDD anode and stainless steel cathode; ultrasound source of low (200W) and high frequency (450W); uv lamp (254 nm); T = 25 °C; J = 12.8 mA $cm^{-2}$. | Complete. | [12] |
| Electrochemical oxidation with GAC adsorption | 120 mg $L^{-1}$ | BDD anode and stainless steel cathode; V = 1 L; T =25 ± 1 °C; J = 20-30 mA $cm^{-2}$. | Complete. | [38] |
| ZVI, electrolysis and photolysis | 30 mg $L^{-1}$ | [ZVI] = 45 g $L^{-1}$;BDD and DSA anode; UV lamp (11 W); V = 1 L; Room temperature; J = 50 mA $cm^{-2}$ | Complete with BDD anode. | [28] |
| Electrodialysis and electro-oxidation | 100 mg $dm^{-3}$ | BDD and MMO anodes; NaCl and $Na_2SO_4$ as supporting electrolytes; J = 177.7 A $m^{-2}$; V = 1 $dm^3$. | Higher removal rates for the BDD anode. | [39] |
| Photoelectrolysis | 100 mg $dm^{-3}$ | Novel laser-prepared mixed metal oxide (MMO $RuO_2TiO_2$) NaCl (3.7 g $L^{-1}$) and $Na_2SO_4$ (3 g $L^{-1}$) as supporting electrolytes j=30 A $m^{-2}$; V = 150 mL. | Non total removal. MMO more effective in NaCl media | [40] |

In this case, it has also evaluated the kinetics of the combined process, mineralization decay, identification of transformation products to conclude with the discussion of tentative degradation pathways proposed for each technology studied, in order to shed light on the treatability of such wastes, which allows a more efficient design of future applications.

## 2. Material and Methods

123    **Chemical reagents.** All chemicals were purchased of reagent grade and used as

124    received. Clopyralid - $C_6H_3Cl_2NO_2$, 99 % purity, solubility > 1 g $L^{-1}$ at 20°C, $K_{ow}$ =

125    $2.34^{-3}$ at pH 7 and 20°C (a.r., Sigma-Aldrich) was selected as a model of organic

126    compound. Iron zero valent, ≥ 99%, granular, 10-40 mesh, average size is 568 µm.

127    Methanol HPLC grade and formic acid were used as mobile phase. Sodium sulphate

128    anhydrous used as supporting electrolyte. These chemicals were purchased from Sigma-

129    Aldrich, Spain). Sulfuric acid (98%), sodium hydroxide pellets (97%) were obtained

130    (a.r., Scharlab, Spain) and used to control pH. Double deionized water (Millipore Milli-

131    Q system, resistivity: 18.2 MΩ cm at 25ºC) was used to prepare all solutions.

132    **Experimental set-up.** In order to evaluate the efficiency of the combined technologies,

133    four strategies were developed. The first one consists of applying single electrochemical

134    treatment employing a single flow cell (SFC) using boron-doped diamond electrodes

135    with 78 $cm^2$ of area as anode and cathode (WaterDiam, France). A 1.5 L glass reactor

136    was filled with 1 L of water containing 30 mg $L^{-1}$ of clopyralid and 7.04 mM of

137    $Na_2SO_4$. The electro-oxidation was carried out galvanostatically by applying a current

138    density of 50 mA $cm^{-2}$ as it was explained elsewhere [27]. The second strategy consists

139    of a photochemical treatment using the same set up described early coupled to UV lamp

140    of 11W and wavelength of 254 nm. UV lamp is a cylinder tube of 15 cm of length and

141    10 mm of diameter and it was 80% covered by water in a vertical position. UV light

142    was irradiated directly to the tank without applying any electrical current. The combined

143    strategies consist of the pre-treatment of the waste for 72 h with 45 g $L^{-1}$ of ZVI (stirring

144    rate 300 rpm) followed by application of photolysis or electrolysis process as described

145    above. Optimum experimental conditions for ZVI dehalogenation were determined in

146    preliminary experiments as described elsewhere [34]. Before the application of AOPs

147    processes, clopyralid solutions were filtered with 0.45 µm Nylon Supelco filters to

148   avoid the possible iron suspended particles generated in the dehalogenation process. All

149   experiments were conducted for 240 minutes and samples were taken at defined times

150   along the experiments. Temperature of the system was kept constant (25ºC) by means of

151   a thermostatic bath (JP Selecta, Digiterm 100) and a heat exchanger. The monitored

152   parameters were pH and conductivity of the solution, total organic carbon (TOC),

153   clopyralid concentration and intermediates generated.

154   **Analytical techniques**

155   Selected samples were collected and filtered with 0.22 µm Nylon Supelco filters before

156   analysis. The quantification of the clopyralid and some dehalogenated intermediates were

157   carried out by HPLC (Agilent 1200 series) using a ZORBAX Eclipse Plus5 C18

158   analytical column. The mobile phase consisted of 30% methanol / 70% water with 0.1%

159   of formic acid (flow rate: 0.8 mL min$^{-1}$). The DAD detection wavelength was 280 nm, the

160   retention time around 2.6 min, the temperature was maintained 25ºC and the injection

161   volume was 20 µL. The TOC concentration was monitored using a Multi N/C 3100

162   Analytic Jena Analyser. The evolution of the pH and conductivity were determined by a

163   pH meter Crison pH25+ and a conductometer Crison CM35+ (Crison Instruments,

164   Spain), respectively. Both instruments were calibrated regularly with standard solutions

165   and all the samples were measured in duplicate. The reactions intermediates of clopyralid

166   were identified by Liquid Chromatography-Mass Selective Detector (LC-MSD) using a

167   Zorbax SB-C18 (150mm×4.6 mm, 3.5 µm particle size) column (Agilent Technologies

168   CA, USA). Detection was carried out with a UV–Vis diode array detector (DAD) at 230

169   and 280 nm (Agilent, 1260 infinity model) equipped with a flow cell coupled in series to

170   an Agilent 6110 series MS detector (Waldbronn, Germany) equipped with an

171   atmospheric pressure ionization source electrospray (API-ES).  Selected samples were

172   analyzed using the ESI interface in positive ionization (PI) mode. For the analysis in PI

173  mode a gradient elution was performed by a binary gradient, composed of solvent A

174  (water/0.1% HCOOH) and solvent B (acetonitrile/0.1% HCOOH) according to the

175  following program: initial conditions 80% A, kept constant for 1 min, decreased to 50%

176  in 4 min, decreased to 20% in 6 min, kept constant for 8 min, returned to the initial

177  conditions after 2 min. Re-equilibration time was set at 2 min, while the total run analysis

178  lasted 10 min. Column temperature was set at 25°C, injection volume and flow rate were

179  1000 μL and 1 mL min$^{-1}$, respectively. To optimize the MS detection of each analyte, the

180  drying gas flow was investigated within the 1.0–13.0 L min$^{-1}$. The temperature of the

181  drying gas was also studied in a range from 50 to 350°C. The capillary voltage ranged

182  from 2000 to 6000 V. Additionally, the nebulizer pressure, ranged from 5.0 to 60 psi, and

183  the fragmentor from 50 to 200.

184

185  **3.     Results and discussion**

186  Fig. 1 shows the evolution of clopyralid and TOC as a function of time in the four

187  treatment technologies evaluated in this work. Regarding herbicides decay (Fig. 1a), the

188  photolytic process exhibited very low removal attaining only 10%. Although the

189  pesticide absorbs UV light, the efficiency of this kind of treatment depends on many

190  factors like UV fluence, irradiation time, molecule structure, etc. In the case of

191  clopyralid structure, as discussed by Wilzbach and Rausch, 1970 [41], even though

192  there is a presence of a heteroatom and an aromatic system in its structure, the

193  photochemical dissociation mechanism of the pyridine ring is through of the n/p*

194  excitation, leading to a bicyclic valence isomer, Dewar pyridine, which re-aromatizes

195  completely to pyridine in a few minutes at room temperature. This important

196  phenomena was also discussed by Semitsoglou-Tsiapou et al, that showed that

197  clopyralid (55 mL containing 20 mg L$^{-1}$) was hardly susceptible to low-pressure

photolysis, achieving only 1.2% of removal, although it follows the same mechanism [36].

Similarly, the treatment with ZVI particles for 72 h led to a slight decrease in the clopyralid removal (around 5 %). To understand this value, it is important to consider that the pesticide concentration in this work is higher than that used in others works in the literature. Thus, Correia et al 2013 [42], studied the 2,4-D degradation by ZVI and showed around 50% degradation was achieved in the presence 2% w/v of ZVI after 150 min. However, when photolysis was applied after the ZVI process, the degradation of pesticide was accelerated, increasing the rate of removal from 5% to 58%. This behavior can be explained in terms of the presence of oxygen (mixing kept for 72 h) during the ZVI treatment, which allows to transform the ZVI reducing conditions into oxidative reactions. Thus, oxygen reacts with ZVI generating $O_2^{2-}$, which can react further through two routes. The reduction of $O_2$ through a 4e$^-$ pathway with production of $H_2O_2$ as an intermediate and a 2 e$^-$ pathway, with formation of $H_2O_2$ as product. From this point of view, the efficiency of oxidative degradation of clopyralid depends on the extent to which the branching process favors hydroxyl radical formation by reduction of $H_2O_2$ through 2e$^-$pathway[42]. Thus, the photo-assistance in the UV promotes the Fenton reaction, yielding $^\bullet$OH. Furthermore, studies previous [43, 44] suggest that the photo radiation in the presence of ZVI can promote ZVI/$O_2$ reaction to produce HO$\bullet$ as shown following Eqs. (1) and (2) , enhancing the process efficiency

$$Fe^0 + O_2 + 2H+ \rightarrow Fe(II) + H_2O_2 \tag{1}$$

$$Fe(II) + H_2O_2 \rightarrow Fe(III) + OH^- + HO\bullet \tag{2}$$

On the other hand, results demonstrate that the single EO process is a suitable technology for the clopyralid removal, being able to oxidize completely the pesticide

after 180 min of treatment (current charge of 1.6 Ah dm$^{-3}$). Considering the cell voltage, this means that the energy consumed in the process was only 11.46 kWh m$^{-3}$. These results are expected considering the formation of hydroxyl radical on the surface of the anode, which will be discussed later. In addition, other oxidants are expected to be formed with this technology and as reported in the literature, when sulfate radicals are present in the medium, they can be transformed into persulfate [45-47]. These electrogenerated oxidant species may produce mediated oxidation in the bulk solution, complementing the mechanisms of oxidation and contributing to an increase in global oxidation efficiency. In order to expedite the electro-oxidation, previous treatment with ZVI particles was added to this technique. The addition led to slight improvement of the process performance, decreasing the time to attain the complete herbicide removal.

Fig. 1b shows the performance of the treatment techniques regarding to the mineralization of the solution. As can be seen, the single ZVI treatment does not provide significant mineralization (only 5%). Photolysis, as well, yields only 10% mineralization after 180 min. Despite ZVI + photolysis improved the degradation of CLP, the mineralization only reached 22%. This behavior can be attributed to the dechlorination of the CLP, which makes the structure more vulnerable to photolysis. On the other hand, despite EO and ZVI + EO were able to attain complete CLP degradation, around 20% of initial TOC still remained in the solution. This means that organic content corresponds to the degradation by-products of CLP. However, the ZVI + EO process was found to give a remarkable improvement in the mineralization, increasing the efficiency from 4.3 to 4.9 mg TOC (Ah)$^{-1}$.
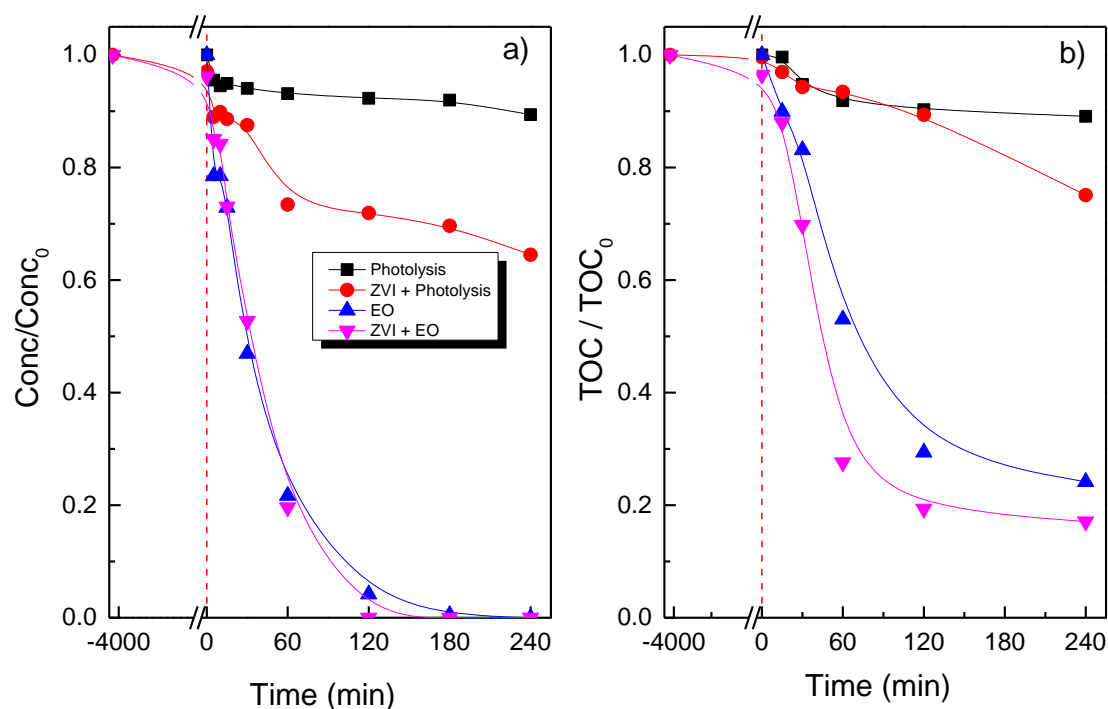
**Figure 1.** Relative removal of Clopyralid and b) Relative TOC decay as a function of

time during the (■) photolysis; (●) ZVI + photolysis, (▲) EO and (▼) ZVI + EO.

Concentration and TOC decay were fitted to a ~~pseudo~~ first-order kinetics, and values are

reported in the Fig. 2a. As expected, values obtained for ZVI process were very low (in

the range of $10^{-7}$ $min^{-1}$) for both CLP and TOC removal. Photolytic process also

presents low reaction rate ($10^{-4}$ $min^{-1}$), albeit higher as compared to ZVI process. When

light is applied, a significant improvement is observed ($10^{-4}$ to $10^{-2}$ $min^{-1}$), explained in

terms of an increase in hydroxyl radical production stemming from the photolysis of

$H_2O_2$, which accelerates the oxidation rate of all organic compounds present in the

medium and contributes to the optimization of the process performance. Besides, ZVI +

EO process shows a higher increasing of the amount of hydroxyl radicals and other

oxidants formed on the BDD surface and in the bulk (such as persulfates, ozone and

peroxide species). On the other hand, analyzing the mentioned combined process ~~ZVI+~~

260 EO, it is possible to see that k values for CLP oxidation and mineralization did not

261 increase with the pre-treatment with ZVI. Nevertheless, a significant improvement is

262 observed in the mineralization when electrooxidation using diamond electrodes is

263 assessed in comparison with photolytic processes. This behavior suggests a constant

264 electrolytic production of $^\bullet OH$ radicals from reaction (3), which acts mainly in the

265 oxidation of byproducts in the bulk.

266
$$H_2O \rightarrow {}^\bullet OH + H^+ + e^- \tag{3}$$

267 In order to evaluate quantitatively the synergistic effect when two or more process are

268 combined, the synergistic index was calculated from kinetics values according to eq. 4.

269
$$Sinergistic\ index\ (S) = \frac{k_{ZVI+PHOTO}}{K_{ZVI} + k_{PHOTO}} \tag{4}$$

270 Figure 2b shows the synergistic index of the combined system obtained for ~~2,4-D~~ CLP

271 and TOC removal. The first combined process (ZVI + photolysis) is called S1 while the

272 combination ZVI+ EO is called S2. Synergy index values >1 indicate that there is a

273 synergism effect when process is combined. Considering the clopyralid removal, the

274 values obtained from Eq. (4) yields a synergistic index of 5.1 for S1 and 10.1 for S2,

275 indicating a strong synergistic effect for ~~2,4-D~~ CLP removal and both hybrid process.

276 However, S values equal to 0.93 and 1.2 were obtained for S1 and S2 for TOC decay

277 indicating an almost nil synergistic effect for mineralization. These results indicate that

278 ZVI is acting in the transformation of CLP via reductive dechlorination reactions. In

279 this way their concentration decreases significantly. However, after successive

280 elimination of Cl atoms, the ZVI is not able to degrade the more recalcitrant molecule

281 formed to $CO_2$ and water and neither the EO process is able to get a total removal.

282 Then, results indicate that the application of combined process ZVI + EO is not an

283 excellent mechanism for the mineralization of organic compound once the target

284 molecule fails to undergo mineralization, which agrees with our previous results

285 published elsewhere [27].



286
287
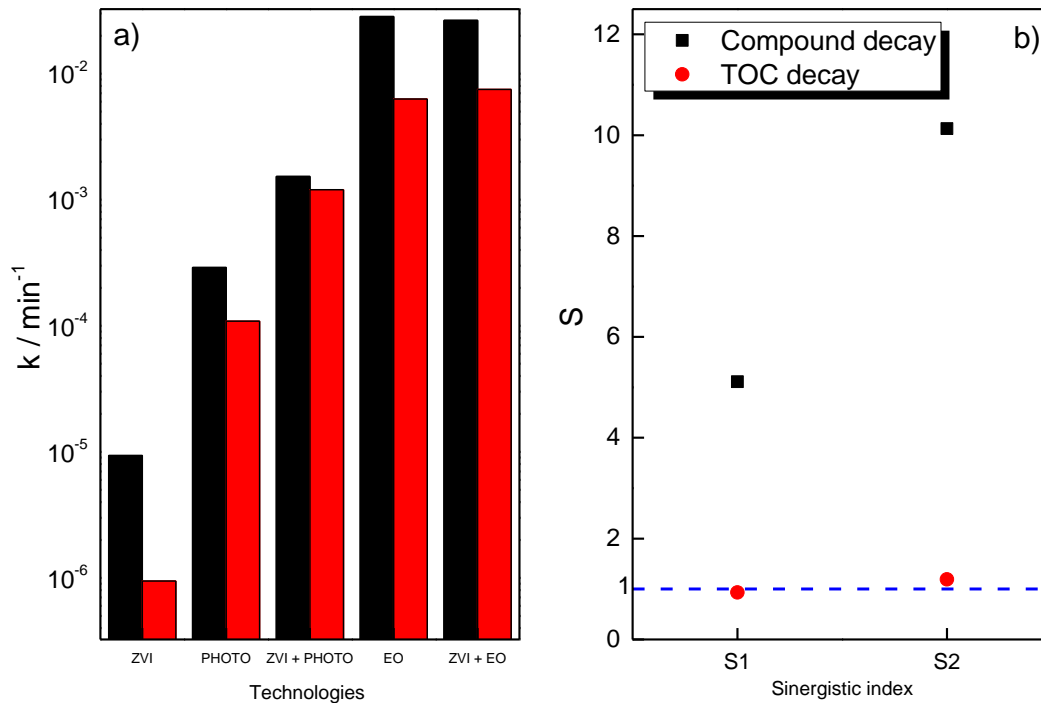
**Figure 2. a)** Kinect constants obtained after fitting the clopyralid and TOC decay

results to a first-order kinetic reaction model. b) Synergistic effect calculated for (■)

compound decay and (●) TOC

291 In Fig. 3, it can be seen the evolution of pH and conductivity during the treatments

292 evaluated. These parameters give an information about the species generated during the

293 treatments. As seen, after 72 h of the ZVI pre-treatment, there is a slight decrease in the

294 solution pH. However, this parameter remained unchanged during the coupled

295 processes (e.g ZVI + photolysis and ZVI+EO). In addition, it was not observed the

296 formation of iron hydroxides and just low concentration of iron (II) ions and chloride

297 were obtained according with eq (5) because of the low hydroxyl ions released during

the whole pre-treatment proposed. However, further research should be necessary to know more about these iron products.

$$Fe^0 + 2H_2O \rightarrow Fe^{2+} + H_2 + 2OH^- \tag{5}$$
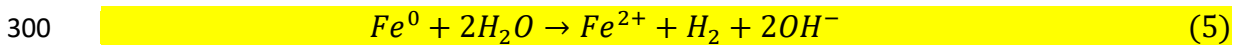
Then, this indicates that reduction reactions can promote the generation of mildly acid species. During the photolytic process, the pH remained stable. This behavior was expected since considerable changes were observed in the treatment process (as observed in the Fig.1ab). The remarkable change in the pH was observed after the electro-oxidation process, for which there is an increase of pH from 5.2 to 9.5. In terms of conductivity, their changes were negligible over the whole reaction period in the photolysis and ZVI + photolysis processes. However, the values significantly increased during the electro-oxidation processes. This can be explained not only by the changes in the pH but also in terms of the larger generation of oxidant species, initially produced through a low concentration of $H_2O_2$ generated prior to the efficient radicals promoted by EO processes as it was suggested by Minella et al.[48] at slightly acid pH.
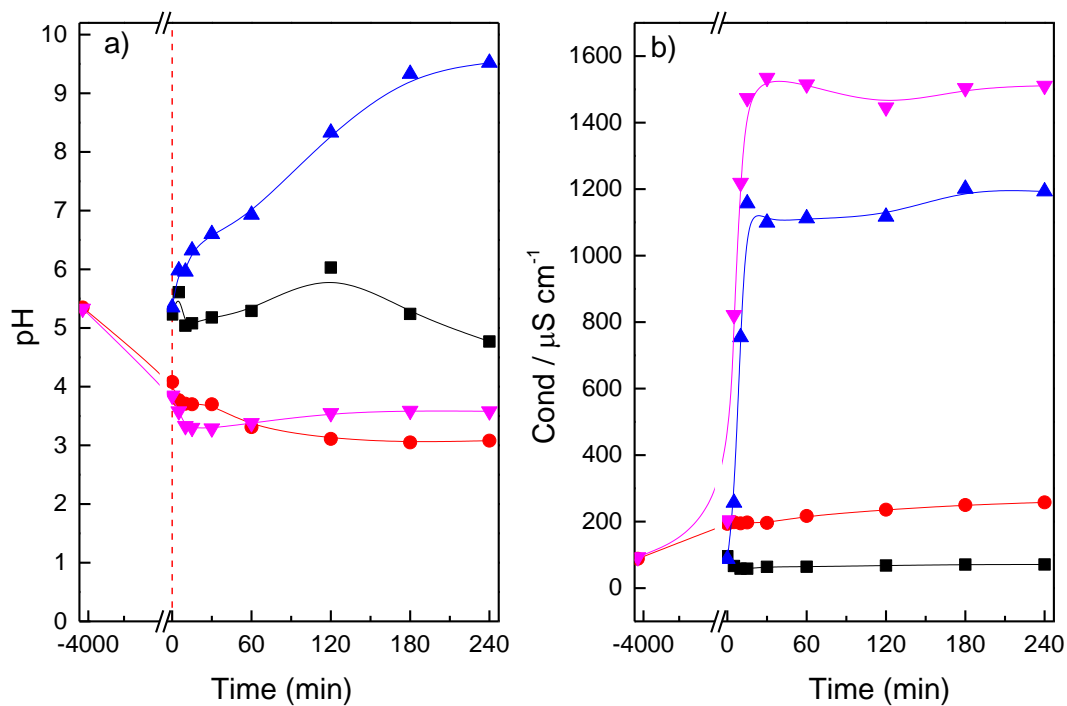
**Figure 3. a)** pH and b) Conductivity evolution as a function of time during the (■) photolysis, (●) ZVI + photolysis, (▲) EO and (▼) ZVI + EO.

Fig. 4 shows the HPLC chromatograms of the processed samples in the four evaluated processes. It can be observed the higher peak is related to Clopyralid at retention time 2.8 min. Besides, a very short number of byproducts appear in chromatograms. This may be a reflection of the low concentration of the byproducts generated. It is possible to see two important reaction products in retention times at 1.0 and 1.4 min. Both peaks appear during the photolytic process, being the most relevant at 1.4 min. However, in the ZVI + photolysis (fig.4b) this peak is lower than in photolysis and quickly disappears. Fig, c shows that during the EO technology, CLP was destroyed within few minutes of reaction. The byproduct at 1.4 min was not found and the peak at 1.0 min is negligible. In the presence of ZVI particles as pre-treatment of the EO process, it can be

326　observed (Fig.4d) that the compound at 1.0 min is continually removed, decreasing their

327　concentration with the time.



328
329
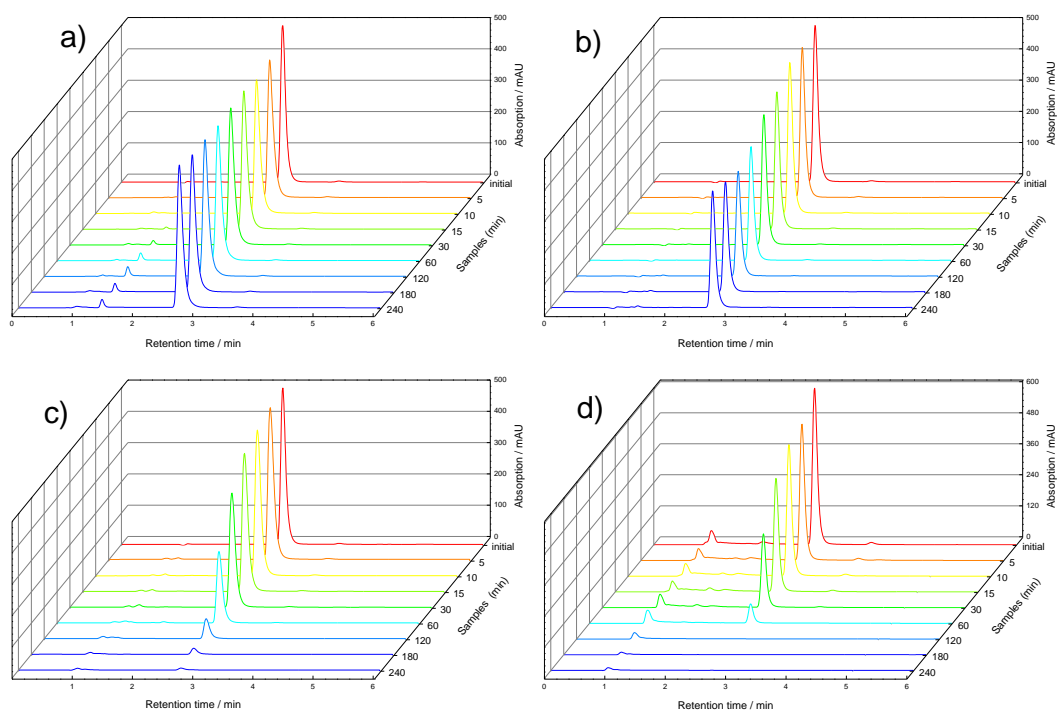
**Figure 4.** Chromatograms obtained from HPLC analysis for each sample taking during

a) photolysis process; b) ZVI + photolysis; c) EO process and d) ZVI + EO. (Eluent:

water with 0.1% formic acid and acetonitrile 30: 70 v/v; flow rate: 1 cm$^3$ min$^{-1}$, Vol.

inj.: 20 μL; Column: Zorbax Eclipse Plus 5 C18, 30 cm; λ = 280 nm; Temp. 25 ºC)

334

These two important by-products were identified based on the literature and throughout

of internal standard method. Peaks were quantified with external standard calibration

based on areas from the standard reagents. The by-product at 1.0 min was identified as

pyridine- 2-carboxylic acid and the product at 1.4 min as 6-chloro-3-hydroxypyridine-2-

carboxylic acid. As it can be seen in the Fig.5ab, both concentrations are very low. One

340 important point to <mark>be considered</mark> is the fact that the both products mainly appears after

341 using the ZVI as pre-treatment. The pyridine-2-carboxilic acid concentration (Fig.5a)

342 decreases with time when UV irradiation is coupled to ZVI process. Besides, it is

343 completely oxidized within 50 minutes of electro-oxidation (ZVI+EO). Regarding to 6-

344 chloro-3-hydroxypyridine-2-carboxylic acid (Fig.5b), its concentration remains

345 unchanged over time when ZVI + photolysis process was accomplished. This behavior

346 means that this product is more refractory, and <mark>it does not undergo</mark> photolytic cleavage

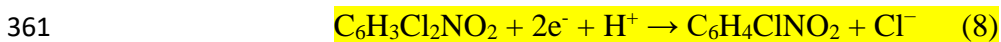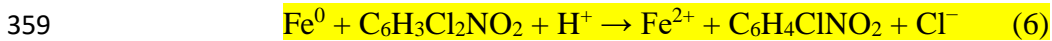347 easily. However, it is completely degraded with ZVI+EO process.
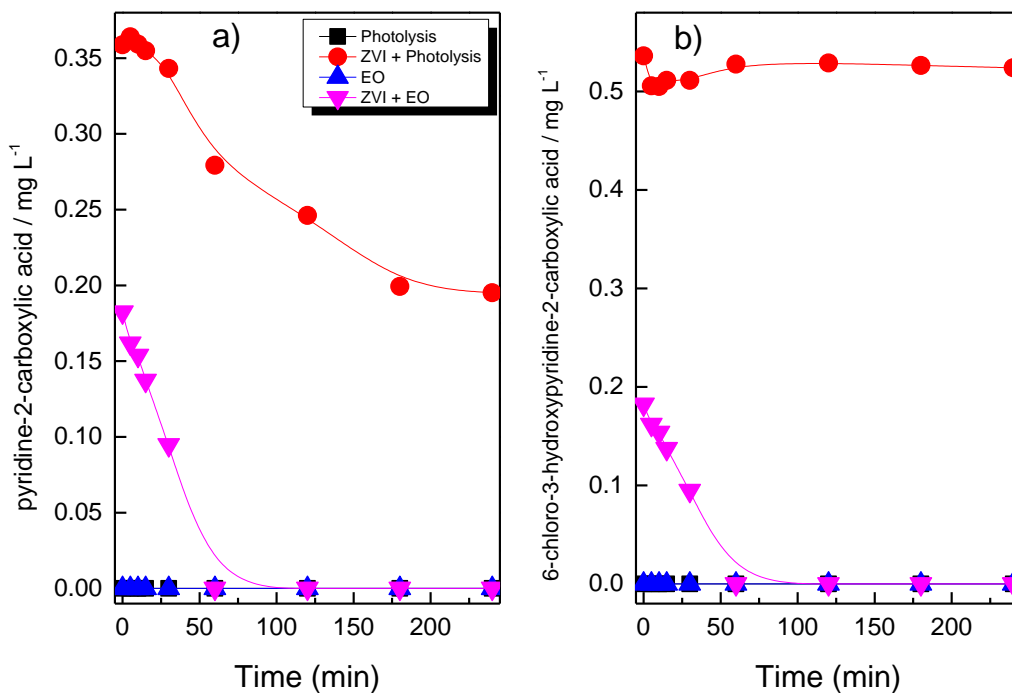


348
349

350 **Figure 5**. Intermediates evolution as a function of time during the (■) photolysis; (●)

351 ZVI + photolysis, (▲) EO and (▼) ZVI + EO. a) pyridine-2-carboxylic acid and b) 6-

352 chloropyridine-2-carboxylic acid.

353 <mark>Formation of these dehalogenated species is known to be carried out by reductive</mark>

354 <mark>chemical processes catalyzed by the iron particles (heterogeneous catalytic reaction) as</mark>

355 shown in eqs. 6 and 7 or by cathodic hydro-dehalogenation reactions, which should lead

356 to the formation of the same intermediates but without production of iron (II) ions (eqs.

357 8 and 9) [34]

358

359 $$Fe^0 + C_6H_3Cl_2NO_2 + H^+ \rightarrow Fe^{2+} + C_6H_4ClNO_2 + Cl^- \qquad (6)$$

360 $$Fe^0 + C_6H_4ClNO_2 + H^+ \rightarrow Fe^{2+} + C_6H_5NO_2 + Cl^- \qquad (7)$$

361 $$C_6H_3Cl_2NO_2 + 2e^- + H^+ \rightarrow C_6H_4ClNO_2 + Cl^- \qquad (8)$$

362 $$C_6H_4ClNO_2 + 2e^- + H^+ \rightarrow C_6H_5NO_2 + Cl^- \qquad (9)$$

363

364 The LC -MS analyses carried out at a negative ion mode was used for the identification

365 of the degradation products. Firstly, the conditions of the mass detector were optimized.

366 The best results obtained when the drying gas was operated at 12 L min$^{-1}$ flow at

367 340°C. The nebulizing pressure at 60 psi, capillary voltage at 5000 V and the

368 fragmentation voltage was set at 70 V (for PI ionization). Then, samples collected at

369 regular time intervals were injected into the MS analysis in mode scan at different

370 ranges, being set at two channels 1 and 2. The products identified, as well their

371 structure, retention time and sampling time of the process and % relative abundance for

372 each technology are showed in Table 2. As it can be observed, the analyzed samples

373 during the four investigated treatments indicated the formation of several intermediates.

374 During the photolytic process, four reaction products were identified. This means that

375 the UV irradiation was able to break chemicals bonds: the photonic energy absorbed

376 exceeded the bond energy as radiation at 254 nm which even has more energy than the

377 necessary to break the C–Cl bond (dissociation energy is 330 kJ mol$^{-1}$) and which may

378 promote further reactivity. Those compounds were 2,5-dichloropyridine (m/z = 148),

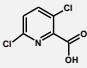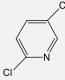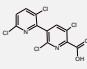379 2',3,5',6-tetrachloro[2,3'-bipyridine]-6'-carboxylic acid (m/z = 337), 3,6-dichloro-
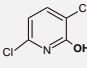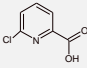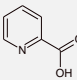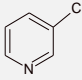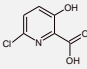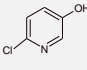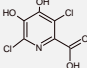
380   pyridine-2-ol (m/z = 163) and 6-chloropyridine-2-carboxylic acid (m/z = 157). These

381   intermediates were also found during the ZVI + photolysis process. However, two more

382   products were identified: pyridine-2-carboxylic acid (m/z = 122) and 3-chloropyridine

383   (m/z = 113). Considering that these molecules have lower molecular weight than those

384   obtained during the photolytic treatment, this means that the oxidations steps achieved

385   superior levels, confirming the improvement obtained for the ZVI + photolysis process

386   in the oxidation of the solution.

387   The largest number of intermediates was found for the ZVI+ EO process. As it can be

388   observed, two hydroxylated species were observed during the EO and ZVI+ EO

389   processes. These byproducts are 3,6-dichloro-4,5-dihydroxypyridine-2-carboxylic acid,

390   m/z = 224 at retention time tr= 11.0 min and 3,6-dichloro-5-hydroxypyridine-2-

391   carboxylic acid, m/z = 207 at tr 9.4 min (set at channel#2). At this point, it is worthy of

392   note that during the electro-oxidation processes using BDD anodes are expected to be

393   produced an enormous amount highly active and non-selective oxidizing species, the

394   $^{\bullet}$OH radicals (HRs) [49, 50]. Also, it is known that one of the major mechanistic steps

395   of $^{\bullet}$OH radicals (HRs) treatment is the hydroxylation of organic compounds, especially

396   of unsaturated bonds, through hydrogen substitution or hydroxyl addition [51-53].

397   However, as discussed above, not only $^{\bullet}$OH radicals (HRs), but others powerful

398   oxidants species also acts in the oxidation process. Then, smaller molecules are formed.

399   In the case of EO process, the products were slightly different than those obtained when

400   ZVI was applied as pre-treatment. As can be seen in the Table 2, the main products

401   identified during the EO process were 6-chloro-3-hydroxypyridine-2-carboxylic acid

402   (m/z = 174) and 6-chloropyridin-3-ol (m/z = 128). Conversely, for ZVI + EO process,

403   four more products were found, 3,6-dichloro-pyridine-2-ol (m/z = 164), 6-

404   chloropyridine-2-carboxylic acid (m/z = 157), pyridine-2-carboxylic acid (m/z = 122)

and 3-chloropyridine (m/z = 113). These two last products appeared to be more hydrophilic than the other products, because its retention time in the C18 column was lower than all other compounds, being tr = 3.6 min and tr = 2.8 min, respectively.

**Table 2.** Analytes identified, structure, retention time and sampling time of electrolysis and % relative abundance for each technology.

| Analyte | Structure | tr (min) | m/z | Photo Sampling time (% rel. abundance) | ZVI + Photo Sampling time (% rel. abudance) | EO Sampling time (% rel. abudance) |
|---|---|---|---|---|---|---|
| Clopyralid | | 9.8*2 | 191 | - | - | - |
| 2,5-dichloropyridine | | 5.9 | 148 | 240 (10) | 60 (30) | |
| 2',3,5',6-tetrachloro[2,3'-bipyridine]-6'-carboxylic acid | | 10.3*2 | 337 | 240 (40) | 10 (30) | |
| 3,6-dichloro-pyridine-2-ol | | 4.3*2 | 164 | 180 (10) | 10 (70) | 30 (70) |
| 6-chloropyridine-2-carboxylic acid | | 4.0*2 | 157 | 240 (70) | 10 (100) | |
| pyridine-2-carboxylic acid | | 3.6 | 122 | | 10 (40) | |
| 3-chloropyridine | | 2.8 | 113 | | 10 (40) | |
| 6-chloro-3-hydroxypyridine-2-carboxylic acid | | 9.6*2 | 174 | | | 10 (70) |
| 6-chloropyridin-3-ol | | 3.7 | 128 | | | 60 (60) |
| 3,6-dichloro-4,5-dihydroxypyridine-2-carboxylic acid | | 11.0*2 | 224 | | | 10 (40) |

411

412 Fig. 6 shows a plausive mechanism proposed for CLP degradation based on the peaks

413 observed by LC-MS. The main pathway for each process is marked by dotted coloured

414 lines. The primary pathway of clopyralid degradation by UV irradiation (marked by

415 blue points-via 1), takes place by transfer of one electron to generated radical anion

416    followed by decarboxylation (-COOH) and attack of the $^{\bullet}$OH radical leading to the

417    formation of 3,6-dichloropyridin-2-ol (m/z=164). Another important reaction route is

418    the generation of the dimer 2,3,3,6-tetrachloro(2,3-bypyridine)-6-carboxylic acid. This

419    formation is caused because the clopyralid loses an electron generating a radical

420    cationic species, followed by the loss of a H$^+$ to give a radical species, which reacts with

421    the radical 2,5-dichloropyridine to form the dimer. The dimers generation is related in

422    the literature as result of the fact that the radiation at 254 nm has more energy than

423    needed to break the C–Cl bond, as it has previously commented. This rupture leads to

424    the formation of a chlorine radical and an unpaired electron on the carbon of the organic

425    molecule [54]. Then, the combinations lead to form more stable molecules (e.g dimers).

426    Similar proposals were also obtained by some other authors applying photocatalysis in

427    the CLP treatments [29, 55].

428    A similar trend in reactivity with ZVI coupled to photolysis was observed as those

429    obtained with only photolysis. However, in this case, more products were identified

430    with higher abundance during the first minutes of reactions. In this way, the main

431    transformation of CLP is proposed to have occurred via sequential reductive

432    dechlorination reactions, forming the monochlorinated product (m/z = 157) that

433    ultimately generated the m/z = 122, which did not contain any Cl atom. In addition, the

434    6-chloropyridine-2-carboxylic acid is attacked by $\cdot$OH radical followed by its

435    decarboxylation (-COOH). Once it is formed, it can be reduced to lead to 3-chloro-

436    pyridine.

437    During the EO process (pathway 3-red line), the primary reaction route, as commented

438    above, is the hydroxylation of the CLP on unsaturated bond of the pyridine ring,

439    through attack of hydroxyl radicals generated on BDD surface. The sequential

440    hydroxylation forms the products of m/z = 207 and with less abundance the m/z = 224.

441  Then, the 3,6-dichloro-5-hydroxypyridine-2-carboxylic acid (m/z = 207) suffers

442  decarboxylation to form the m/z = 164. Another reaction route that can occur is the

443  attack of hydroxyl radical on CLP, which there is the substitution of chlorine specie by

444  hydroxyl radical to form the molecule m/z= 174. From this point, oxidation reaction

445  occurs by attack of hydroxyl radical and other oxidants such as persulfates to generate

446  the decarboxylated product m/z = 128). The oxidative ring-opening reactions follow,

447  possibly to form short-chain carboxylic acids and inorganic ions.

448  The pathway marked by green dotted points is related to ZVI as pre-treatment of the

449  electro-oxidation. As seen, the main products observed at high abundance are those

450  which there is a substitution of Cl species by ·OH, forming the product 6-chloro-3-

451  hydroxypyridine-2-carboxylic acid, followed by decarboxylation via attack of powerful

452  oxidants species. Besides, the products obtained via 4 (EO-red lines) were also

453  identified, meaning that both routes are probable to occur. However, it is worthy to note

454  that albeit both pathways can occur (because products of both pathways were

455  identified), the transformation based on hydroxylation of CLP (via 4) is less important

456  than that of via reaction 3. Finally, these intermediates are degraded to $CO_2$, $H_2O$, $NH_4^+$

457  as it can be postulated on the basis TOC measurement where around 80% of

458  mineralization was attained after about 240 min of electroxidation. Non-mineralized

459  organics can be explained in terms of the formation of iron-carboxylic acid complexes,

460  which are known to be very refractory. However, these potential intermediates were not

461  identified with the analytical techniques used in this work.

462
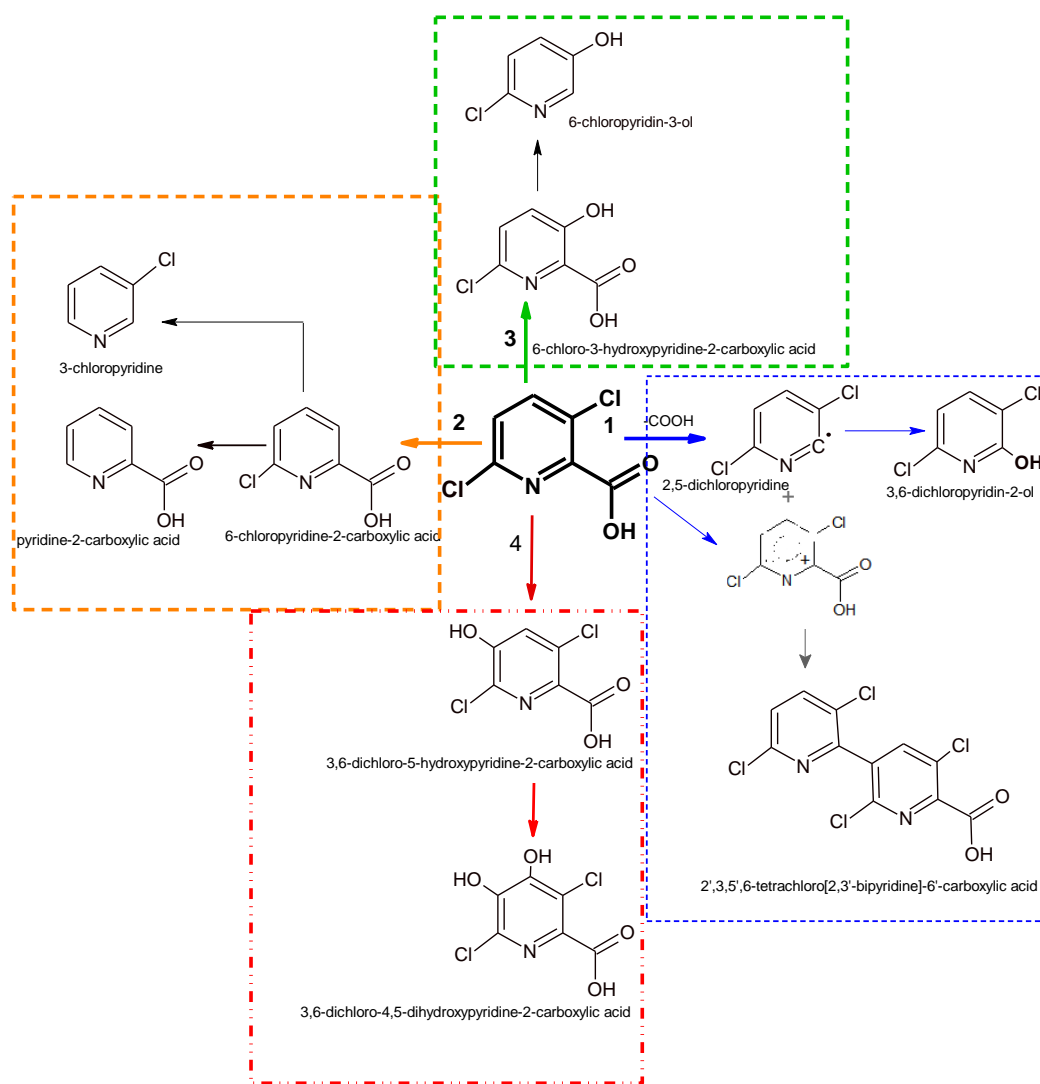


**Figure 6:** Tentative pathways for preferential clopyralid degradation by photolysis (blue), ZVI + photolysis (Orange), electrooxidation (red) and ZVI + EO (green).

**Conclusions**

From this work, the following conclusions can be drawn:

- Single photolysis is not very efficient, and it only attains 5 % of removal of the pollutant. An improvement up to 45 % in the removal is obtained when ZVI was employed as pre-treatment, albeit almost 80 % of organic carbon still remain in the solution after the treatment. Electro-oxidation is an excellent technology to treat clopyralid attaining 100 % of removal and 78% of mineralization within 4

h of reaction. ZVI as pre-treatment of EO was found to be the most efficient technique evaluated for leading more than 80% of total mineralization, slightly improving the results of the single process.

- Higher rates of mineralization were obtained in this order: ZVI + EO > EO > ZVI > photolysis, increasing from a minimum of $10^{-4}$ min$^{-1}$ in single photolysis to $10^{-2}$ min$^{-1}$ in the coupled ZVI + EO process. The synergistic index (S) obtained for the coupled techniques were 5.1 for ZVI+ photolysis and 10.1 for ZVI+EO that indicated a strong synergistic effect for CLP removal. However, the synergy coefficient for the mineralization were very closed to unity for both coupled processes indicating no synergism.

- The identification of transformation products was carried out for each treatment. In total, ten transformation products were identified. Tentative pathways for preferential clopyralid degradation for all processes were proposed shedding light on how occurs the preferential mechanism of each treatment evaluated.

**Acknowledgements**

**References**

498    [1] C.A. Martínez-Huitle, M. Panizza, Electrochemical oxidation of organic pollutants for
499    wastewater treatment, Current Opinion in Electrochemistry, 11 (2018) 62-71.
500    [2] O. Scialdone, Electrochemical oxidation of organic pollutants in water at metal oxide
501    electrodes: A simple theoretical model including direct and indirect oxidation processes at the
502    anodic surface, Electrochim. Acta, 54 (2009) 6140-6147.
503    [3] I. Sirés, E. Brillas, M.A. Oturan, M.A. Rodrigo, M. Panizza, Electrochemical advanced
504    oxidation processes: today and tomorrow. A review, Environmental Science and Pollution
505    Research, 21 (2014) 8336-8367.
506    [4] H. Särkkä, A. Bhatnagar, M. Sillanpää, Recent developments of electro-oxidation in water
507    treatment — A review, Journal of Electroanalytical Chemistry, 754 (2015) 46-56.
508    [5] P. Cañizares, R. Paz, C. Sáez, M.A. Rodrigo, Costs of the electrochemical oxidation of
509    wastewaters: A comparison with ozonation and Fenton oxidation processes, Journal of
510    Environmental Management, 90 (2009) 410-420.
511    [6] I. Linares-Hernández, C. Barrera-Díaz, B. Bilyeu, P. Juárez-GarcíaRojas, E. Campos-Medina, A
512    combined electrocoagulation–electrooxidation treatment for industrial wastewater, Journal of
513    Hazardous Materials, 175 (2010) 688-694.
514    [7] M. Muñoz, J. Llanos, A. Raschitor, P. Cañizares, M.A. Rodrigo, Electrocoagulation as the Key
515    for an Efficient Concentration and Removal of Oxyfluorfen from Liquid Wastes, Industrial &
516    Engineering Chemistry Research, 56 (2017) 3091-3097.
517    [8] J. Llanos, A. Raschitor, P. Cañizares, M.A. Rodrigo, Exploring the applicability of a combined
518    electrodialysis/electro-oxidation cell for the degradation of 2,4-dichlorophenoxyacetic acid,
519    Electrochim. Acta, 269 (2018) 415-421.
520    [9] A. Raschitor, J. Llanos, P. Cañizares, M.A. Rodrigo, Novel integrated electrodialysis/electro-
521    oxidation process for the efficient degradation of 2,4-dichlorophenoxyacetic acid,
522    Chemosphere, 182 (2017) 85-89.
523    [10] M. MuñozMorales, C. Sáez, P. Cañizares, M.A. Rodrigo, A new strategy for the electrolytic
524    removal of organics based on adsorption onto granular activated carbon, Electrochemistry
525    Communications, 90 (2018) 47-50.
526    [11] M. Muñoz-Morales, C. Sáez, P. Cañizares, M.A. Rodrigo, A new electrochemically-based
527    process for the removal of perchloroethylene from gaseous effluents, Chemical Engineering
528    Journal, 361 (2019) 609-614.
529    [12] M.J. Martín de Vidales, M.P. Castro, C. Sáez, P. Cañizares, M.A. Rodrigo, Radiation-assisted
530    electrochemical processes in semi-pilot scale for the removal of clopyralid from soil washing
531    wastes, Separation and Purification Technology, 208 (2019) 100-109.
532    [13] S. Cotillas, E. Lacasa, M. Herraiz-Carboné, C. Sáez, P. Cañizares, M.A. Rodrigo, Innovative
533    photoelectrochemical cell for the removal of CHCs from soil washing wastes, Separation and
534    Purification Technology, 230 (2020) 115876.
535    [14] D. Montanaro, R. Lavecchia, E. Petrucci, A. Zuorro, UV-assisted electrochemical
536    degradation of coumarin on boron-doped diamond electrodes, Chemical Engineering Journal,
537    323 (2017) 512-519.
538    [15] M.J. Martín de Vidales, C. Sáez, P. Cañizares, M.A. Rodrigo, Removal of triclosan by
539    conductive-diamond electrolysis and sonoelectrolysis, Journal of Chemical Technology &
540    Biotechnology, 88 (2013) 823-828.
541    [16] M.J.M.d. Vidales, S. Barba, C. Sáez, P. Cañizares, M.A. Rodrigo, Coupling ultraviolet light
542    and ultrasound irradiation with Conductive-Diamond Electrochemical Oxidation for the
543    removal of progesterone, Electrochim. Acta, 140 (2014) 20-26.
544    [17] M.B. Carboneras, M.A. Rodrigo, P. Canizares, J. Villaseñor, F.J. Fernandez-Morales, Electro-
545    irradiated technologies for clopyralid removal from soil washing effluents, Separation and
546    Purification Technology, 227 (2019) 115728.
547    [18] S. Cotillas, E. Lacasa, C. Sáez, P. Cañizares, M.A. Rodrigo, Electrolytic and electro-irradiated
548    technologies for the removal of chloramphenicol in synthetic urine with diamond anodes,
549    Water Research, 128 (2018) 383-392.

550    [19] J.F. Pérez, J. Llanos, C. Sáez, C. López, P. Cañizares, M.A. Rodrigo, Electrochemical jet-cell
551    for the in-situ generation of hydrogen peroxide, Electrochemistry Communications, 71 (2016)
552    65-68.
553    [20] J.F. Pérez, J. Llanos, C. Sáez, C. López, P. Cañizares, M.A. Rodrigo, The pressurized jet
554    aerator: A new aeration system for high-performance H2O2 electrolyzers, Electrochemistry
555    Communications, 89 (2018) 19-22.
556    [21] H. Olvera-Vargas, X. Zheng, O. Garcia-Rodriguez, O. Lefebvre, Sequential "electrochemical
557    peroxidation – Electro-Fenton" process for anaerobic sludge treatment, Water Research, 154
558    (2019) 277-286.
559    [22] M. Rodríguez, M. Muñoz-Morales, J.F. Perez, C. Saez, P. Cañizares, C.E. Barrera-Díaz, M.A.
560    Rodrigo, Toward the Development of Efficient Electro-Fenton Reactors for Soil Washing
561    Wastes through Microfluidic Cells, Industrial & Engineering Chemistry Research, 57 (2018)
562    10709-10717.
563    [23] L. Teevs, K.D. Vorlop, U. Prüße, Model study on the aqueous-phase hydrodechlorination of
564    clopyralid on noble metal catalysts, Catal. Commun., 14 (2011) 96-100.
565    [24] Z.-Y. Zhang, M. Lu, Z.-Z. Zhang, M. Xiao, M. Zhang, Dechlorination of short chain
566    chlorinated paraffins by nanoscale zero-valent iron, Journal of Hazardous Materials, 243 (2012)
567    105-111.
568    [25] I. San Román, M.L. Alonso, L. Bartolomé, A. Galdames, E. Goiti, M. Ocejo, M. Moragues,
569    R.M. Alonso, J.L. Vilas, Relevance study of bare and coated zero valent iron nanoparticles for
570    lindane degradation from its by-product monitorization, Chemosphere, 93 (2013) 1324-1332.
571    [26] Y. Han, W. Yan, Reductive Dechlorination of Trichloroethene by Zero-valent Iron
572    Nanoparticles: Reactivity Enhancement through Sulfidation Treatment, Environmental Science
573    & Technology, 50 (2016) 12992-13001.
574    [27] C. Carvalho de Almeida, M. Muñoz-Morales, C. Sáez, P. Cañizares, C.A. Martínez-Huitle,
575    M.A. Rodrigo, Electrolysis with diamond anodes of the effluents of a combined soil washing –
576    ZVI dechlorination process, Journal of Hazardous Materials, 369 (2019) 577-583.
577    [28] M.B. Ferreira, M. Muñoz-Morales, C. Sáez, P. Cañizares, C.A. Martínez-Huitle, M.A.
578    Rodrigo, Improving biotreatability of hazardous effluents combining ZVI, electrolysis and
579    photolysis, Science of The Total Environment, (2020) 136647.
580    [29] D.V. Sojic, V.B. Anderluh, D.Z. Orcic, B.F. Abramovic, Photodegradation of clopyralid in
581    TiO2 suspensions: identification of intermediates and reaction pathways, J. Hazard. Mater.,
582    168 (2009) 94-101.
583    [30] S. Semitsoglou-Tsiapou, M.R. Templeton, N.J.D. Graham, L. Hernández Leal, B.J. Martijn, A.
584    Royce, J.C. Kruithof, Low pressure UV/H2O2 treatment for the degradation of the pesticides
585    metaldehyde, clopyralid and mecoprop – Kinetics and reaction product formation, Water
586    Research, 91 (2016) 285-294.
587    [31] M. Ahmadi, F. Ghanbari, Degradation of organic pollutants by photoelectro-peroxone/ZVI
588    process: Synergistic, kinetic and feasibility studies, Journal of environmental management, 228
589    (2018) 32-39.
590    [32] E. GilPavas, S. Correa-Sánchez, Optimization of the heterogeneous electro-Fenton process
591    assisted by scrap zero-valent iron for treating textile wastewater: Assessment of toxicity and
592    biodegradability, Journal of Water Process Engineering, 32 (2019) 100924.
593    [33] F. Deng, O. Garcia-Rodriguez, H. Olvera-Vargas, S. Qiu, O. Lefebvre, J. Yang, Iron-foam as a
594    heterogeneous catalyst in the presence of tripolyphosphate electrolyte for improving electro-
595    Fenton oxidation capability, Electrochim. Acta, 272 (2018) 176-183.
596    [34] C. Carvalho de Almeida, M. Muñoz-Morales, C. Sáez, P. Cañizares, C.A. Martínez-Huitle,
597    M.A. Rodrigo, Integrating ZVI-dehalogenation into an electrolytic soil-washing cell, Separation
598    and Purification Technology, 211 (2019) 28-34.
599    [35] M.B. Carboneras Contreras, F. Fourcade, A. Assadi, A. Amrane, F.J. Fernandez-Morales,
600    Electro Fenton removal of clopyralid in soil washing effluents, Chemosphere, 237 (2019)
601    124447.

602    [36] S. Semitsoglou-Tsiapou, M.R. Templeton, N.J. Graham, L. Hernandez Leal, B.J. Martijn, A.
603    Royce, J.C. Kruithof, Low pressure UV/H2O2 treatment for the degradation of the pesticides
604    metaldehyde, clopyralid and mecoprop - Kinetics and reaction product formation, Water Res,
605    91 (2016) 285-294.
606    [37] C. Tizaoui, K. Mezughi, R. Bickley, Heterogeneous photocatalytic removal of the herbicide
607    clopyralid and its comparison with UV/H2O2 and ozone oxidation techniques, Desalination,
608    273 (2011) 197-204.
609    [38] M. Muñoz-Morales, C. Sáez, P. Cañizares, M.A. Rodrigo, Enhanced electrolytic treatment
610    for the removal of clopyralid and lindane, Chemosphere, 234 (2019) 132-138.
611    [39] A. Raschitor, J. Llanos, M.A. Rodrigo, P. Cañizares, Is it worth using the coupled
612    electrodialysis/electro-oxidation system for the removal of pesticides? Process modelling and
613    role of the pollutant, Chemosphere, 246 (2020) 125781.
614    [40] G.O.S. Santos, K.I.B. Eguiluz, G.R. Salazar-Banda, C. Saez, M.A. Rodrigo, Photoelectrolysis
615    of clopyralid wastes with a novel laser-prepared MMO-RuO2TiO2 anode, Chemosphere, 244
616    (2020) 125455.
617    [41] K.E. Wilzbach, D.J. Rausch, Photochemistry of nitrogen heterocycles. Dewar pyridine and
618    its intermediacy in photoreduction and photohydration of pyridine, J. Am. Chem. Soc., 92
619    (1970) 2178-2179.
620    [42] A. Correia de Velosa, R. Nogueira, 2,4-Dichlorophenoxyacetic acid (2,4-D) degradation
621    promoted by nanoparticulate zerovalent iron (nZVI) in aerobic suspensions, Journal of
622    environmental management, 121C (2013) 72-79.
623    [43] C. Lee, C.R. Keenan, D.L. Sedlak, Polyoxometalate-Enhanced Oxidation of Organic
624    Compounds by Nanoparticulate Zero-Valent Iron and Ferrous Ion in the Presence of Oxygen,
625    Environmental Science & Technology, 42 (2008) 4921-4926.
626    [44] G. Lyngsie, L. Krumina, A. Tunlid, P. Persson, Generation of hydroxyl radicals from
627    reactions between a dimethoxyhydroquinone and iron oxide nanoparticles, Scientific Reports,
628    8 (2018) 10834.
629    [45] P. Cañizares, C. Sáez, A. Sánchez-Carretero, M.A. Rodrigo, Synthesis of novel oxidants by
630    electrochemical technology, Journal of Applied Electrochemistry, 39 (2009) 2143.
631    [46] J.M. Aquino, M.A. Rodrigo, R.C. Rocha-Filho, C. Sáez, P. Cañizares, Influence of the
632    supporting electrolyte on the electrolyses of dyes with conductive-diamond anodes, Chemical
633    Engineering Journal, 184 (2012) 221-227.
634    [47] F. Souza, S. Quijorna, M.R.V. Lanza, C. Sáez, P. Cañizares, M.A. Rodrigo, Applicability of
635    electrochemical oxidation using diamond anodes to the treatment of a sulfonylurea herbicide,
636    Catalysis Today, 280 (2017) 192-198.
637    [48] M. Minella, E. Sappa, K. Hanna, F. Barsotti, V. Maurino, C. Minero, D. Vione, Considerable
638    Fenton and photo-Fenton reactivity of passivated zero-valent iron, RSC Advances, 6 (2016)
639    86752-86761.
640    [49] B. Marselli, J. Garcia-Gomez, P.A. Michaud, M.A. Rodrigo, C. Comninellis,
641    Electrogeneration of Hydroxyl Radicals on Boron-Doped Diamond Electrodes, Journal of The
642    Electrochemical Society, 150 (2003) D79.
643    [50] I. Duo, A. Fujishima, C. Comninellis, Electron transfer kinetics on composite diamond
644    (sp3)–graphite (sp2) electrodes, Electrochemistry Communications, 5 (2003) 695-700.
645    [51] M.G. Antoniou, J.A. Shoemaker, A.A. de la Cruz, D.D. Dionysiou, LC/MS/MS structure
646    elucidation of reaction intermediates formed during the TiO(2) photocatalysis of microcystin-
647    LR, Toxicon : official journal of the International Society on Toxinology, 51 (2008) 1103-1118.
648    [52] L.P. Cermenati, P.; Guillard, C.; Albini, A., Probing the TiO2 Photocatalytic Mechanisms in
649    Water Purification by Use of Quinoline,Photo-Fenton Generated OH• Radicals and Superoxide
650    Dismutase, J. Phys. Chem. B, 101 (1997) 2650-2658.

651    [53] N. Rabaaoui, K. Saad Mel, Y. Moussaoui, M.S. Allagui, A. Bedoui, E. Elaloui, Anodic
652    oxidation of o-nitrophenol on BDD electrode: variable effects and mechanisms of degradation,
653    Journal of hazardous materials, 250-251 (2013) 447-453.
654    [54] O.S. Keen, E.M. Thurman, I. Ferrer, A.D. Dotson, K.G. Linden, Dimer formation during UV
655    photolysis of diclofenac, Chemosphere, 93 (2013) 1948-1956.
656    [55] C. Berberidou, V. Kitsiou, S. Karahanidou, D.A. Lambropoulou, A. Kouras, C.I. Kosma, T.A.
657    Albanis, I. Poulios, Photocatalytic degradation of the herbicide clopyralid: kinetics, degradation
658    pathways and ecotoxicity evaluation, Journal of Chemical Technology & Biotechnology, 91
659    (2016) 2510-2518.

660